ISSN (Print) 1226-1750
ISSN (Online) 2233-6656
Journal of Magnetics 26(4), 420-426 (2021) https://doi.org/10.4283/JMAG.2021.26.4.420

A Computational Approach to 3-Dimensional Reconstruction Image of Diabetic Foot using the Near-Infrared Spectroscopy (NIRS) after Magnetic Field Intensity Stimulation: Preliminary Study

Sun-Young Cho[1], Ji-Su Park[2], Mezie Laurence B. Ortiz[3]*, and Young-Jin Jung[4]*

[1]*NeuroRehap Inc, Busan 47017, Republic of Korea*
[2]*Advanced Human Resource Development Project Group for Health Care in Aging Friendly Industry, Dongseo University, Busan 47011, Republic of Korea*
[3]*College of Medical Imaging and Therapy, De La Salle Medical and Health Sciences Institute, Cavite 4114, Philippines*
[4]*School of Healthcare and Biomedical Engineering, Chonnam National University, Yeosu 59626, Republic of Korea*

(Received 15 September 2021, Received in final form 26 October 2021, Accepted 26 October 2021)

Diabetes Mellitus (DM) or Diabetes is a disease characterized by a high sugar level in the blood. The foot is considered as a distinct entity where most of the complication arises that often leads to lower extremity amputation. Recently, the Pulse Magnetic Field (PMF) devices that use magnetic field intensity as stimulants are being used to improve blood circulation among patients with peripheral vascular diseases (PVD). This study promotes the use of Near-Infrared Spectroscopy (NIRS) devices in diagnosing and monitoring DM after the use of PMF devices by providing a piece of biomedical evidence through a simulation approach on how to reconstruct a 3-dimensional biological tissue shape models. The result showed that this simulation approach could be of use in the actual reconstruction of a diabetic foot showing the absorption coefficient. NIRS device and the biomedical images could be of use in places where radiographic imaging modalities are not accessible.

Keywords : diabetes, diabetic foot, magnetic stimulation, NIRS, 3D reconstruction

1. Introduction

Diabetes Mellitus (DM) or Diabetes is a metabolic, non-infectious, and non-pathogenic disease characterized by the improper production of insulin by the organ pancreas which results in the abnormal increase in the glucose concentration in the body [1]. DM is considered as a multi-systemic disease that affects individuals of any age, gender, and whatever ethnicity a person belongs [2]. Based on global statistics, in the year 2015, the number of adults suffering from DM accounts for 8.8 % [1] and by the year 2040, there is an estimated projection of 642 million people suffering from this condition which is 10 % of the global population [3]. DM is considered a substantially large and uncontrollable health issue over the next few decades [1].

DM as a disease manifest in every part of the human body. However, it is the musculoskeletal system, in particular, the foot, that is most commonly affected. It involves the lower extremities' skin, soft tissues, muscles, bones and joints, blood vessels and nerves. As stated, it is considered as a distinct entity due to clinical complications detected [2]. Among individuals suffering from DM, 50 % will have diabetic foot infection, 25 % is expected to develop foot ulceration and 84 % of them will undergo lower extremity amputation. The progressive character of the disease demands accurate diagnosis and needs effective management [1,4]. The inability to diagnose the disease upon its onset will lead to major morbidity to the patient including lower extremity amputation. Moreover, over-diagnosis can post a socioeconomic challenge to its governance due to the unwise use of healthcare resources. [4].

Currently, glucometers that invasively measure the blood glucose concentration are being used for monitoring [1]. Also, it is undeniably true that the section of nuclear medicine and radiology addresses the increasing demands of health care, in particular, the need for diagnosis, disease

*Co-corresponding author: Tel: +82-61-659-7366
Fax: +82-0504-211-6134, e-mail: yj@jnu.ac.kr
Tel: +82-63-91-6206-0278, Fax: +82-63-02-988-3100
e-mail: mbortiz@dlshsi.edu.ph

prevention, pathophysiological understanding, and treatment possibilities [5]. Moreover, in the year 1979, the Pulse Magnetic Field (PMF) non-invasive devices were approved by FDA to be used for bone fractures and stimulation of neurons in the brain to promote depolarization or hyper-polarization. Lately, PMF gained popularity as a non-invasive medical treatment for peripheral vascular disease. Several pieces of research in the year 1900's reported that PMF stimulation can increase blood flow. The erythrocytes which are commonly known as red blood cells (RBCs) which consist mainly of hemoglobin deliver oxygen to the body tissues through blood flow in the circulatory system. The aggregation of RBCs is said to be the reason for the reduction of blood flow for it causes an increase in vascular resistance during circulation. In the year 2015, the effect of magnetic field intensity and PMF simulation time in an aggregation of red blood cells in the hand and feet are studied by Hwang, et al concluding the same results. The study reported that a minimum 10 minutes' disaggregation was found in 20 minutes of stimulation time which increases the cell mobility up to 150 seconds. Also, from 0.07 T to 0.19 T the disaggregation of cells was maintained which showed the improvement of the blood flow in vascularity [6].

Looking back, 2 years before the approval of Pulse Magnetic devices, in 1977, a non-invasive and non-ionizing technique known as Near-Infrared Spectroscopy (NIRS) was being utilized in which the major events were initiated by Frans Jöbsis who is considered as the founder of Vivo NIRS. During his post-doctoral degree at the University of Pennsylvania, he focused on monitoring of intact tissues with the use of non-invasive optical properties. Specifically, he demonstrated that during hyperventilation, the changes in cortical oxygenation among adults can be detected using NIRS. From this major event, this led to other human functional NIRS application and development up to the present [7].

NIRS an optical method uses near-infrared (NIR) light ranging from 650-1000 nm that enables imaging of the soft tissues of the body that maps the optical properties' spatial and temporal distribution that corresponds to the oxygenated and deoxygenated hemoglobin concentration [8]. Several studies also showed that NIRS allows the determination of the compression and expansion of blood vessels and identification of wound healing potential while maintaining its characteristics as being non-invasive, non-ionizing and easy to use for it does not require manual calibration, no need for additional medical supplies, no need for specifically trained personnel and it is portable. It's mentioned characteristics and usage, allows NIRS to be used as a clinical translational tool in diagnosing and monitoring foot diabetes [9]. Over the years, medical images have a very important role among clinicians in terms of diagnosis and treatment. One of the oldest is the use of X-ray were other tomographic modalities were developed such as Computed Tomography (CT), Magnetic Resonance Imaging (MRI), SPECT, PET or ultrasound [10]. In this paper, the researchers would like to promote the use of NIRS as a non-invasive tool in diagnosing and monitoring the disaggregation of red blood cells after the use of the PMF device by showing a piece of evidence in diagnosing and monitoring this condition after the magnetic field stimulation, a simulation approach on how to reconstruct the 3 Dimensional (3D) biological tissue such as rectangular and realistic shape models will be demonstrated. These biomedical images are oxygenated dynamic images that are reconstructed using the contact-based NIRS. The NIRS device could be of use in remote areas where diagnostic and monitoring devices and radiographic imaging modalities are inaccessible like the PET-CT scan due to its high cost. Moreover, the 3D reconstructed biomedical images could be of use by the clinician for the exploration of the medical condition.

2. Materials and Methods

The Toast++ and MATLAB R2018b software applications are used in this study to show the differences between the assumed 3D biological tissue rectangular and realistic models. Toast++ is an open-source toolbox developed primarily for optical modeling of light transport in tissue and image reconstruction in Diffuse Optical Tomography (DOT). This allows the measurement and visualization of an organ based on the optical properties. The absorption and scattering properties are related to the hemoglobin concentration and metabolism of the tissues that make it a functional imaging tool [11]. The reconstruction of images in DOT involves the forward and inverse problem. In forward problem, the diffusion equation is used to predict the distribution or propagation of NIR light in biological tissue based on the presumed parameters of the source and object while the inverse solver uses the forward problem. The inverse solver reconstructs the distribution of optical properties in the area of interest within the boundaries of light transmission measurement [12]. The MATLAB software application permits the access of Toast++ software through a set of functions that allowed the researchers to manipulate the mesh functions, matrix assembly, and solution without comprising the performance of the toolbox [11].

On this reconstruction approach, the researchers decided to make two biological tissues shape models which are

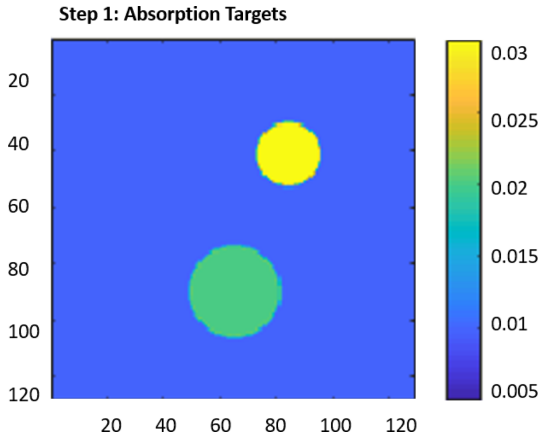

Fig. 1. (Color online) It is the assumed 2D Biological Tissue Model with two targets to show the different absorption coefficients when NIR propagates through a medium. The general parameters set were the refractive index having a value of 1.4, speed of light in a vacuum which is 3×10^8 m/second, and the speed of light in a medium which is the value of the resultant quotient of the speed of light in a vacuum over the refractive index.

the rectangular and realistic models to show comparison and to consider variances in the foot shape especially when there is a presence of wound ulcer for this affects photon absorption per unit path length.

The following are the steps employed to reconstruct 3D biological tissue shape models.

a. Created an assumed biological tissue in a 2D form showing two different absorption targets or nodal coefficients as shown on the color map values (Fig. 1). The absorption targets will serve as the region of interests. The general parameters set were the refractive index having a value of 1.4, speed of light in a vacuum which is 3 × 108 m/second, and the speed of light in a medium which is the

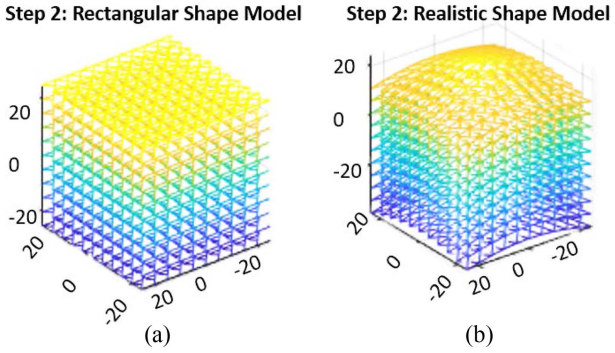

Fig. 2. (Color online) From the 2D Biological Tissue Model created, a 3D biological tissue (a) rectangular and (b) realistic shape models were reconstructed. The 3D biological tissue rectangular shape model was transformed into a realistic shape model by adding an equation changing the z-axis.

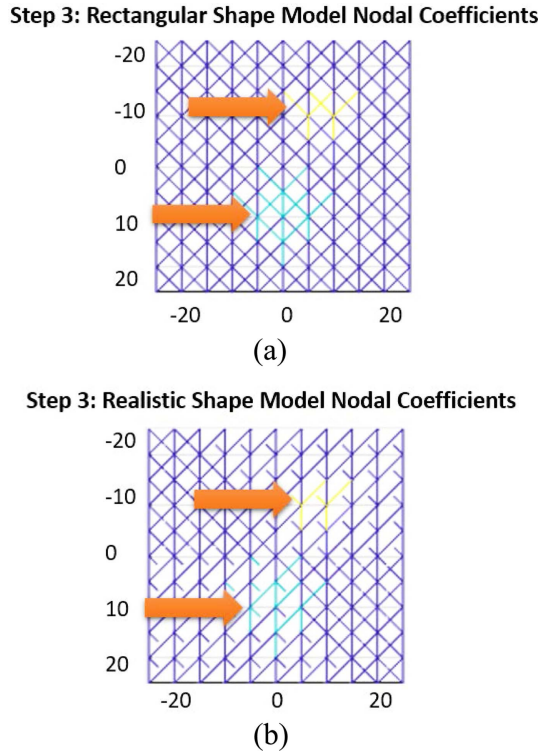

Fig. 3. (Color online) In the created 3D biological tissue (a) rectangular and (b) realistic shape models, two circular targets or nodal coefficients were inserted in the 3D biological tissue rectangular and realistic shape models in which the size of the radius is 25 having different absorption coefficients.

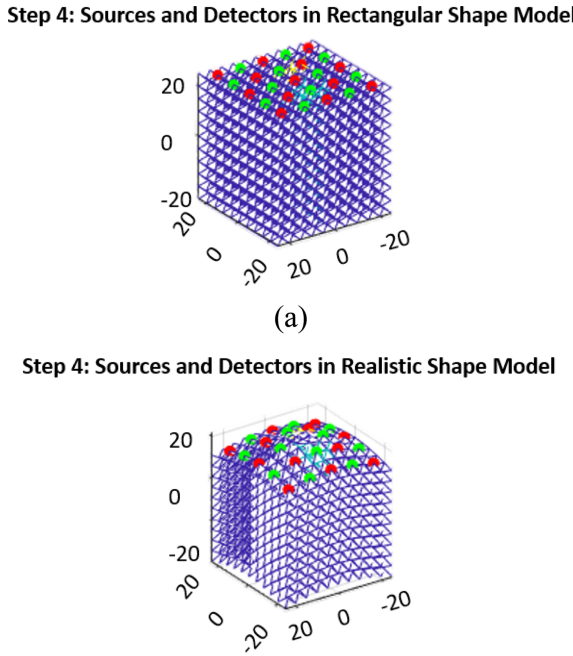

Fig. 4. (Color online) After the 3D reconstruction, Placed 13 sources (red) and 12 detectors (yellow-green) in the 3D biological tissue rectangular and realistic shape models.

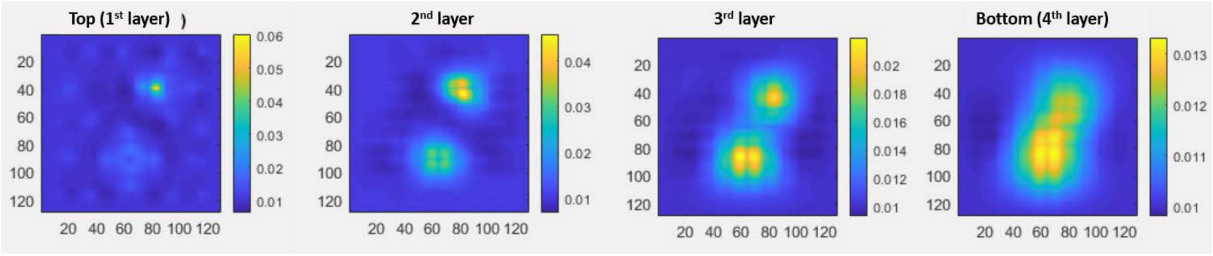

Fig. 5. (Color online) The reconstructed layers of the 3D Biological Tissue Rectangular Shape Model with NIR absorption coefficient values (top view). In the rectangular model, the targets on the top (1st layer) have the highest NIR coefficient ranging from 0.01 to 0.06, followed by the second layer which absorbs 0.01 to 0.04, next is 3rd layer having 0.01 to 0.02 and the bottom (4th layer) with 0.01 to 0.013 values.

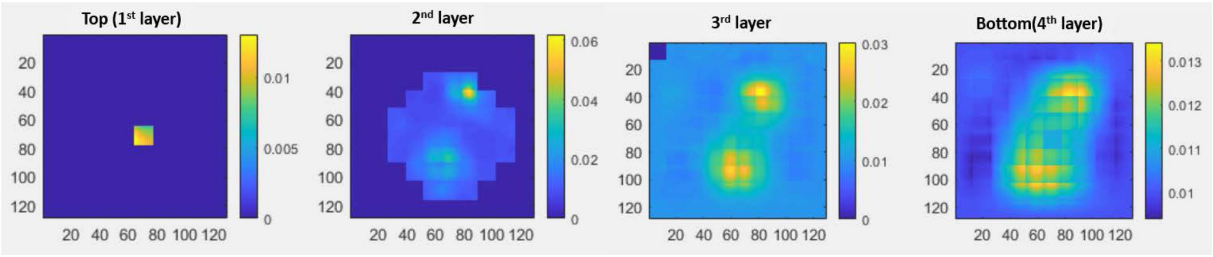

Fig. 6. (Color online) The reconstructed layers of the 3D Biological Tissue Realistic Model with NIR absorption coefficient values (top view). In the realistic shape model, 2nd layer has the highest value of 0 to 0.6, followed by the 3rd layer having 0 to 0.03, next is the bottom (4th layer) with 0.01 to 0.013 and lastly, the top (1st layer) that absorbs 0 to 0.1 NIR absorption coefficient value.

value of the resultant quotient of the speed of light in a vacuum over the refractive index.

b. Reconstructed the assumed 2D biological tissue model into 3D biological tissue rectangular and realistic shape models with equal axis measuring 20 × 20. The 3D biological tissue rectangular shape model was transformed into a realistic shape model by adding an equation changing the z-axis (Fig. 2).

c. Inserted two circular targets or nodal coefficients in the 3D biological tissue rectangular and realistic shape models in which the size of the radius is 25 having different absorption coefficients (Fig. 3).

d. Placed 13 sources (red) and 12 detectors (yellow-green) in the 3D biological tissue rectangular and realistic shape models (Fig. 4). DOT system works by illuminating the NIR light on biological tissue surface at different points and measuring the transmitted light on the tissue and emitted from the boundary through the detectors [11].

3. Results

To illustrate the differences on the result of the simulation approach, 4 layers for each model are exhibited on this paper and named as the top (1st) layer, 2nd layer, 3rd layer, and bottom (4th) layer (Fig. 5, 6, 7, and 8). Note that in MATLAB software application, these reconstructed images are in live-action showing the actual propagation of NIR light. To show a sample of NIR absorption coefficient values, a set of reconstructed images without changing the color map limit was included (Fig. 5 and 6). However, in the succeeding figures, the limit was set to 0 as the minimum and 0.6 for the maximum value to better visualize and differentiate the absorption of NIR among the layers (Fig. 7 and 8).

3.1. Biological Tissue Rectangular and Realistic Shape Models NIR Absorption Coefficient Values

As shown in Fig. 5 in the rectangular model, the targets on the top (1st layer) has the highest NIR coefficient ranging from 0.01 to 0.06, followed by the second layer which absorbs 0.01 to 0.04, next is 3rd layer having 0.01 to 0.02 and the bottom (4th layer) with 0.01 to 0.013 values. Since the shape in all layers is the same, as the NIR propagates through the biological tissue it is continuously attenuated. As NIR light interacts in biological tissues which is a highly scattering medium, the light photons have undergone multiple events of scattering before it is measured by the detectors [11]. However, in the realistic shape model, 2nd layer has the highest value of 0 to 0.6, followed by the 3rd layer having 0 to 0.03, next is the bottom (4th layer) with 0.01 to 0.013 and lastly, the top (1st layer) that absorbs 0 to 0.1 NIR

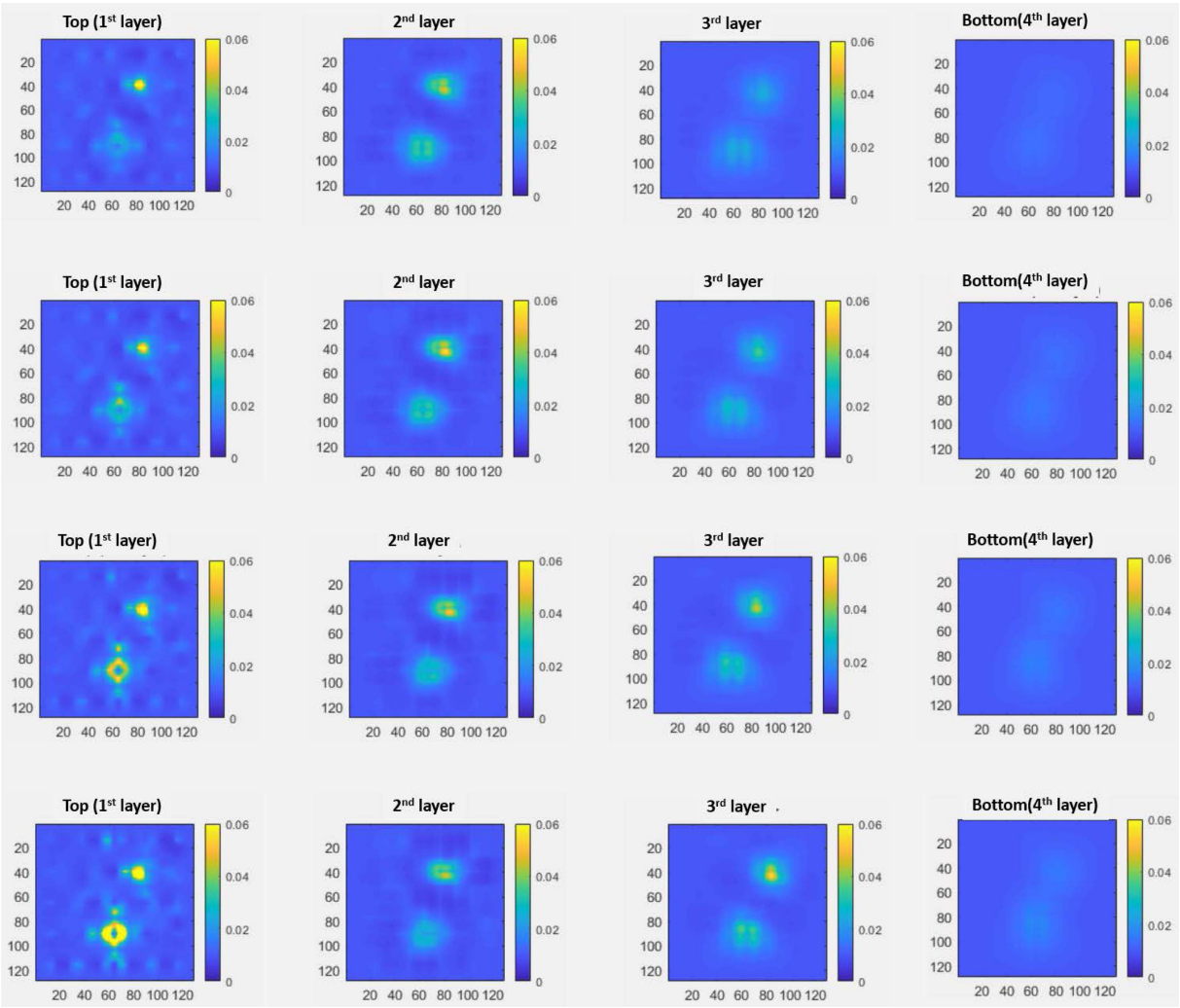

Fig. 7. (Color online) The reconstructed layers of the 3D Biological Tissue Regular Shape Model (top view). The consistency can be noted that the targets are mostly visualized on the top (1st) layers appearing as a yellow circular image and continue to disappear on the succeeding layers almost having the appearance of watermark on the bottom (4th) layers.

absorption coefficient value (Fig. 6). The curvature shape of the model affects the thickness consistency of the biological tissues as well as the propagation of NIR light. Moreover, the smaller the size of the target per reconstructed layers the lesser the chromophores present, therefore the lesser amount of absorber of NIR light.

3.2. Correlation of Biological Tissue Shape Models NIR Absorption Coefficient Values to Reconstructed Layers Visualization

On the assumed 3D biological tissue rectangular model (Fig. 7), the consistency can be noted that the targets are mostly visualized on the top (1st) layers appearing as a yellow circular image and continue to disappear on the succeeding layers almost having the appearance of watermark on the bottom (4th) layers. Moreover, the target areas on the last row are mostly seen than the other rows. Biological tissue NIR absorption coefficient values are directly proportional to target areas visualization. As mentioned, the principle is based on the capability of chromophores to absorb diffusive light at a specific wavelength. The 1st (top) layers have the highest absorption coefficient for it is located in superficial areas while 4th (bottom) layers have the lowest absorption coefficient since it is located in deep-seated areas.

In a realistic model (Fig. 8), it's shape is thick at the center and gradually decreasing towards its periphery. The target areas are mostly visualized on the 2nd, followed by the 3rd, then the bottom (4th), and the top (1st) layer had the least visualized target areas. Also, comparing the rows, it is the last where targets are seen. As the shape of the model changes, the presence of the

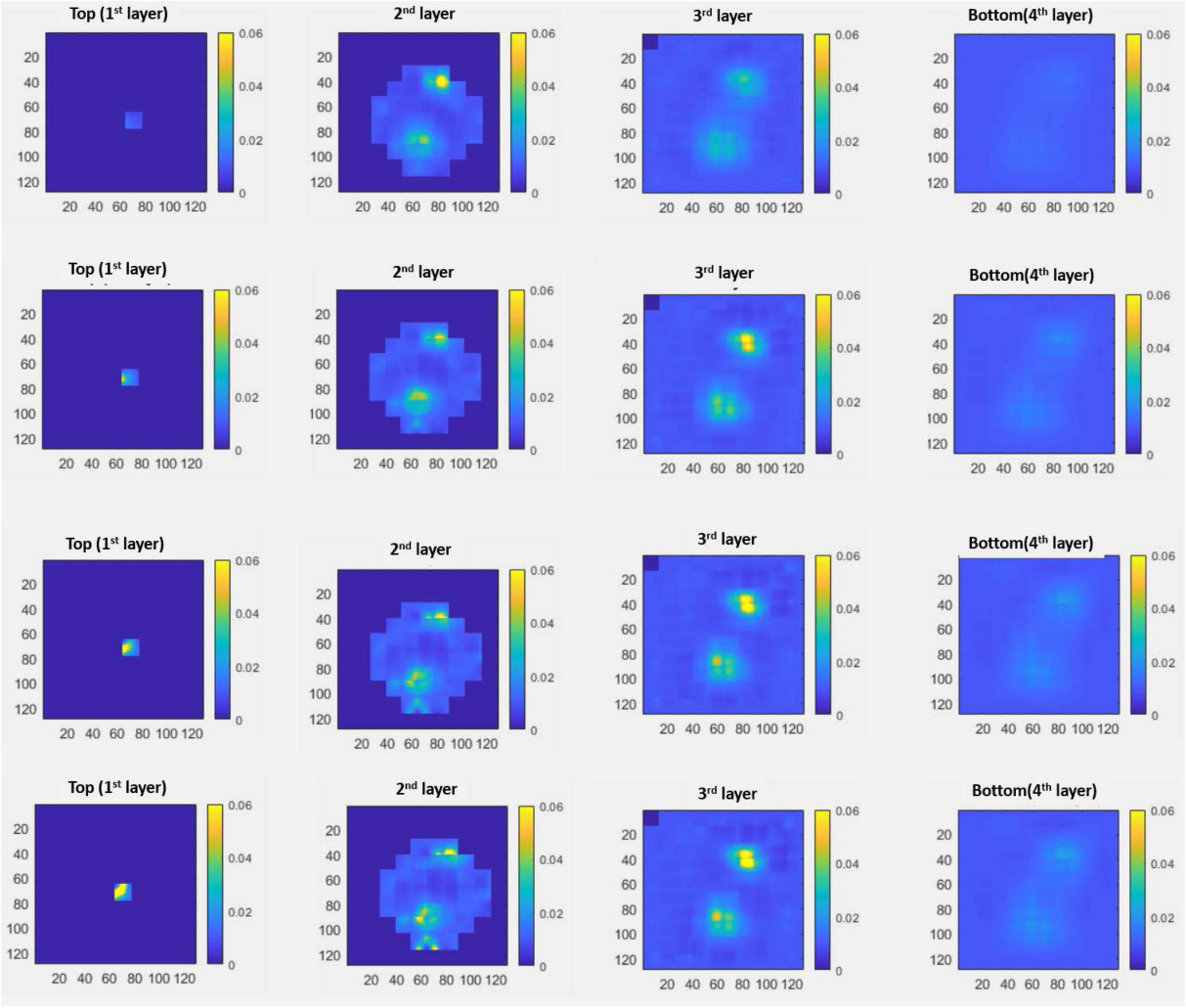

Fig. 8. (Color online) The reconstructed layers of the 3D Biological Tissue Realistic Shape Model (top view). The shape is thick at the center and gradually decreasing towards its periphery. The target areas are mostly visualized on the 2nd, followed by the 3rd, then the bottom (4th), and the top (1st) layer had the least visualized target areas. Also, comparing the rows, it is the last where targets are seen.

chromophores and the scattering properties changes as well and this affects the NIR coefficient values and the reconstructed layers visualization for these two are directly proportional with each other.

4. Conclusion

The NIRS device and the 3D biomedical images reconstructed using Toast++ and MATLAB 2018b software applications could be of use in diagnosing and monitoring the aggregation and disaggregation of RBCs after the stimulation of magnetic field intensity using the PMF devices. Moreover, from the reconstructed images, different NIR absorption coefficient values can also be obtained on each reconstructed layers. These values are affected by several factors and one of those is the shape of the model considering that biological tissues are highly scattering medium. NIR coefficient values are also directly proportional to the visualization of target areas. From an approach to produce 3D reconstructed images, this could be of use in providing the actual 3D reconstructed oxygenated dynamic imaging model of the diabetic foot while segmenting the skin, the soft tissues, the bones, and the vessels to better illustrate the propagation of NIR light in a diabetic foot.

Compliance with Ethical Standards

Conflict of interest - The authors declare no conflict of interest. Human and animal rights This article does not

contain any studies performed on human participants or animals.

Acknowledgment

This research was supported by Basic Science Research Program through the National Research Foundation of Korea (NRF) funded by the Ministry of Education (NRF-2019R1I1A1A01052893) & supported by the Bio & Medical Technology Development Program of the National Research Foundation (NRF) funded by the Korean government (MSIT) (No. 2021M3A9E4081266); This work was supported by the BB21+ Project in 2021.

References

[1] P. M. Arabi, S. Nigudgi, T. Bhat, and A. Ahmed, In 8th International Conference on Computing, Communications and Networking Technologies, ICCCNT 2017. Institute of Electrical and Electronics Engineers Inc.
[2] I. K. Roug and C. Pierre-Jerome, Euro. J. Radio. **81**, 1625 (2012).
[3] N. Peterson, J. Widnall, P. Evans, G. Jackson, and S. Platt, Foot Ankle Int. SAGE Publications Inc. (2017, January 1)
[4] G. Shagos, P. Shanmugamsundaram, A. Varma, S. Padma, and M. Sarma, Indian J. Nucl. Med. **30**, 97 (2015).
[5] A. W. J. M. Glaudemans, A. M. Quintero, and A. Signore, Eur. J. Nucl. Med. Mol. Imaging. **39**, 745 (2012).
[6] D.-G. Hwang, H. Park, W. Kim, J. Lee, and H. S. Lee, Appl. Phys. **117**, 17d156 (2015).
[7] M. Ferrari and V. Quresima, NeuroImage **63**, 921 (2012).
[8] A. Godavarty, Y. Khandavilli, Y.-J. Jung, and P. S. S. Rao, Progress in Biomedical Optics and Imaging – Proceedings of SPIE. 9318 (2015).
[9] M. L. B. Ortiz and Y.-J. Jung, J. Magn. **23**, 559 (2018).
[10] N. Alireza, S. M. R. Mohd, A. Ayman, S. Tanzila, E. R. Abdolvahab, R. Amjad, and U. Mueen, IETE Technical. Review **31**, 199 (2014).
[11] M. Schweiger and S. Arridge, J. Biomed. Opt. **19**, 040801 (2014).
[12] L. V. Wang and H.-I. Wu, New Jersey: John Wiley & Sons, Inc. Print. (2007).